Simulation of ultra-short channel HEMTs with different gate concepts by 2D/3D-hydrodynamic models

Roland Stenzel, Jan Höntschel and Wilfried Klix

University of Applied Sciences Dresden, Friedrich-List-Platz 1, D-01069 Dresden, Germany,
Phone: +49-351-462 2548, Fax: +49-351-462 2193, Email: stenzel@et.htw-dresden.de

Abstract *– Numerical simulations of $In_{0.52}Al_{0.48}As/In_{0.7}Ga_{0.3}As/InP$ HEMTs have been carried out with a 2D/3D-hydrodynamic model. The investigation of double gate and striped-channel devices with the same layer structure results in an increase of cut-off frequencies. At a reduce of gate lengths down to 5 nm short channel effects becomes important in particular for the single gate device. Transistors with alternative gate structures can suppress these effects and improve simultaneously the RF-behavior. At a gate length L_G = 5 nm transit frequencies of about 690 GHz, 790 GHz and 890 GHz can be attained with the single gate, striped-channel and double gate HEMT, respectively. Double pulse-doped devices can achieve THz transit frequencies.*

Keywords : HEMTs, InAlAs/InGaAs/InP, numerical simulation, short channel effects

1. INTRODUCTION

Short channel effects attain increasing importance in novel In-based high electron mobility transistors (HEMTs) at reduced gate lengths in the range less then 100 nm, if increasing cut-off frequencies are aspired. On the other hand novel gate concepts are able to suppress short channel effects and to improve device performance. In this paper we report about numerical simulations of HEMTs with different gate structures. The simulations have been carried out by our 2D/3D-simulator SIMBA. A brief description of the simulation model is represented in section 2. After the presentation of the physical model, which was used for the simulations, a single gate HEMT structure [1] with 25 nm gate length (L_G) was calculated as a reference structure and for a calibration of the model parameters. The same layer structure and the same gate lengths are used in a double gate HEMT similar to nanoscale MOS concepts [2] as well as in a striped-channel HEMT [3]. Furthermore the gate lengths of these structures are reduced down to 5 nm and static and dynamic simulations have been carried out.

2. SIMULATION MODEL

The numerical simulations are realized by the hydrodynamic model of the 2D/3D-simulator SIMBA [4], [5], based on a three-dimensional coupled solution of Poisson equation

$$\nabla\cdot(e\ \nabla j) = -q\left(p - n + N_D^+ - N_A^-\right) \tag{1}$$

the continuity equations for holes and electrons

$$\nabla\cdot\boldsymbol{J}_p = -q\cdot(R - G + \partial\ p/\partial t) \tag{2}$$

$$\nabla\cdot\boldsymbol{J}_n = \ q\cdot(R - G + \partial\ n/\partial t) \tag{3}$$

the transport equations

$$\boldsymbol{J}_p = -qm_p p\cdot\nabla\left(j - Q_p + \frac{kT_p}{q}\right) - m_p\cdot kT_p\cdot\nabla p \tag{4}$$

$$\boldsymbol{J}_n = -qm_n n\cdot\nabla\left(j + Q_n - \frac{kT_n}{q}\right) + m_n\cdot kT_n\cdot\nabla n \tag{5}$$

the energy balance equations

$$\nabla\cdot\boldsymbol{S}_p = \boldsymbol{J}_p\cdot\boldsymbol{E} - \frac{3}{2}kp\frac{(T_p - T_L)}{t_{wp}} - \frac{3}{2}k\frac{\P}{\P t}(pT_p) - \frac{3}{2}kT_p(R - G) \tag{6}$$

$$\nabla\cdot\boldsymbol{S}_n = \boldsymbol{J}_n\cdot\boldsymbol{E} - \frac{3}{2}kn\frac{(T_n - T_L)}{t_{wn}} - \frac{3}{2}k\frac{\P}{\P t}(nT_n) - \frac{3}{2}kT_n(R - G) \tag{7}$$

and the energy transport equations

$$\boldsymbol{S}_p = -k_p\cdot\nabla T_p + \frac{5}{2}\cdot\frac{kT_p}{q}\cdot\boldsymbol{J}_p \tag{8}$$

$$\boldsymbol{S}_n = -k_n\cdot\nabla T_n - \frac{5}{2}\cdot\frac{kT_n}{q}\cdot\boldsymbol{J}_n \tag{9}$$

For the energy relaxation times a model after [6] was used. The discretization of the system of partial differential equations is done by a modified finite differences method (box method). The equation system is solved for the variables j, p, n, T_p, T_n with the Gummel iteration algorithm.
From the results of the static and dynamic simulations a computation of the small-signal parameters is done by calculation of the y-parameters as a function of frequency with the help of recursive relations (Fourier transformation). In consideration of external layout

capacities and resistors the RF-parameters current gain (h_{21}), maximum stable gain (MSG) and maximum available gain (MAG) as well as the transit frequency (f_T) and the maximum frequency of oscillation (f_{max}) can be calculated.

3. RESULTS AND DISCUSSION

First a simulation of an pulse-doped $In_{0.52}Al_{0.48}As$/ $In_{0.7}Ga_{0.3}As$/InP HEMT [1] with a gate length L_G = 25 nm was done. The essential part of the single gate (SG) device used for the simulation is represented in Fig. 1. The 2DEG mobility in the $In_{0.7}Ga_{0.3}As$ channel is 10000 cm^2/Vs at room temperature. The gate-to-channel spacing of the recessed gate amounts 4 nm. For the source and drain contacts resistive regions with typical values of 0.03 Ω·mm are assumed.

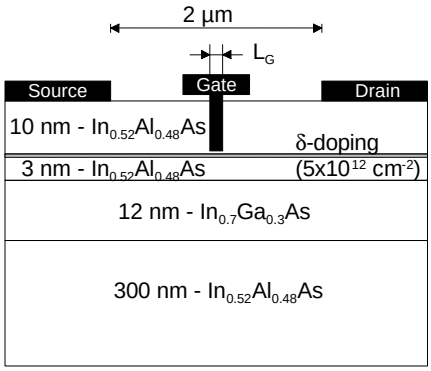

Figure 1: Single gate HEMT structure

Fig. 2 shows the calculated output characteristics as well as measured results [1]. The threshold voltage amounts about -0.4 V. The maximum transconductance of $g_{m,max}$ = 1300 mS/mm corresponds to the experimental value (1230 mS/mm).

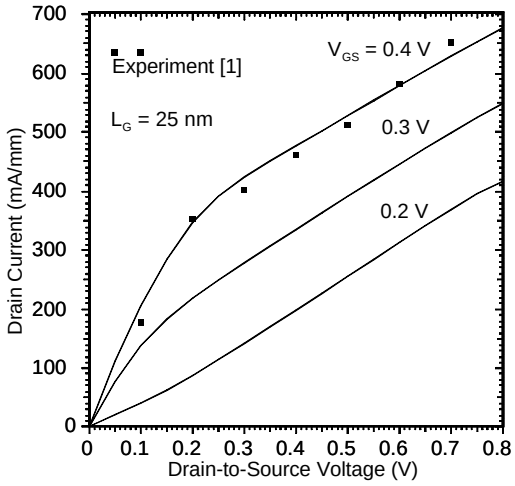

Figure 2: Output characteristics (SG-HEMT)

The RF-gains are plotted in Fig. 3 in comparison with experimental data. The calculated cut-off frequencies f_T = 570 GHz and f_{max} = 350 GHz agree with the measured values f_T = 560 GHz and f_{max} = 330 GHz.

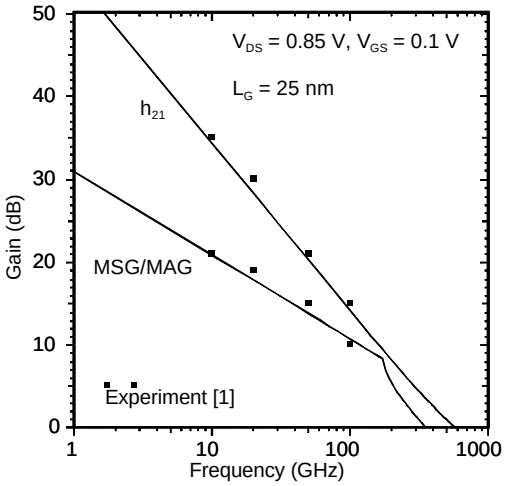

Figure 3: RF-gains vs. frequency (SG-HEMT)

As alternatives to the SG-HEMT, transistors with different gate structures have been investigated. The double gate (DG) HEMT has an additional bottom gate at the backside of the channel, which could be fabricated by a replacement process similar to [2]. The relevant part of the structure used for the simulation is depicted in Fig. 4.

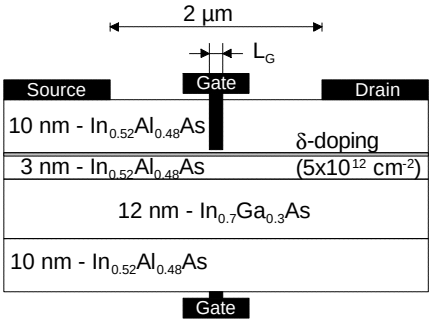

Figure 4: Structure of the double gate (DG) HEMT

For the bottom gate a gate-to-channel aspect ratio of 2.5 was assumed. At the striped-channel (SC) HEMT the gate width (W_G) is limited to small values at both sides of the third device direction by an additional gate recess (similar to [3]). So a horizontal electron confinement (1DEG-like behavior) occurs. For the device a parallel connection of several stripes is done. Fig. 5 shows the cross section of the device (one strip) in the centre of the gate.

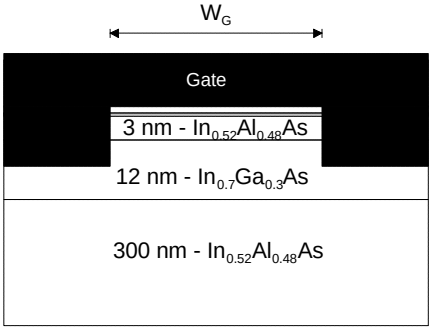

Figure 5: Structure of the striped-channel (SC) HEMT

Due to the symmetry only half of this structure was used for the simulation. For the gate width a value $W_G = 100$ nm was assumed. In this case a 3D simulation is necessary. The output characteristics of the HEMTs with the three different gate structures are represented in Fig. 6.

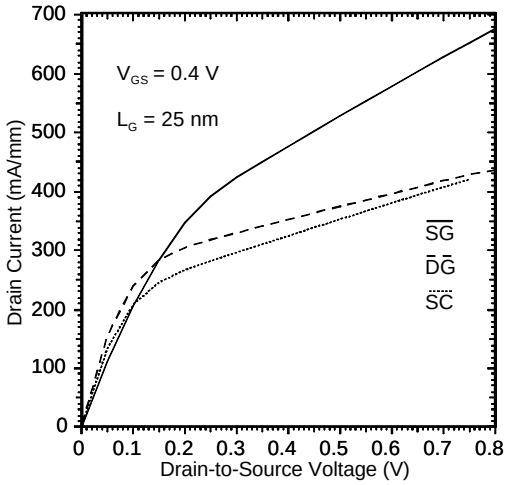

Figure 6: Output characteristics for the different gate types

The short channel effects (saturation output conductance) are reduced obviously for the DG- and SC-HEMT due to the enhanced charge control. The threshold voltage increases from V_{Th} = -0.4 V for the SG-HEMT to 0 V (SC-HEMT) and 0.15 V (DG-HEMT). Furthermore the maximum of transconductance rises from about 1350 mS/mm to 1600 mS/mm and 2550 mS/mm for the SG, SC and DG device, respectively. Consequently an improved RF-performance of the double gate and striped-channel transistors compared to the single gate device can be determined. The cut-off frequencies amount f_T = 590 GHz, f_{max} = 480 GHz (SC-HEMT) and f_T = 640 GHz, f_{max} = 530 GHz (DG-HEMT).

In the following the gate lengths of the different structures are reduced to 15 nm, 10 nm and 5 nm. Due to the very short gate-to-channel spacing (4 nm) of the recessed top gate, this distance remains unchanged. The gate-to-channel aspect ratio of the bottom gate (DG-HEMT) is hold on the constant value 2.5. Fig. 6 - Fig. 9 represent the output characteristics for the different gate lengths at each case for single gate, striped-channel and double gate device. In particular at gate lengths in the range of 10 nm and smaller the saturation behavior of the SG-HEMT (Fig. 6) disappears and the pinch-off characteristic is diminished. Saturation behavior of the striped-channel HEMT can be recognized also at L_G = 10 nm (Fig. 8), whereas the double gate transistor (Fig. 9) results in the best suppression of short channel effects. In Fig. 10 the threshold voltage is represented as a function of the gate length for the different structures. The alternative gate constitutions can be avoid large threshold voltage drops at smaller gate lengths.

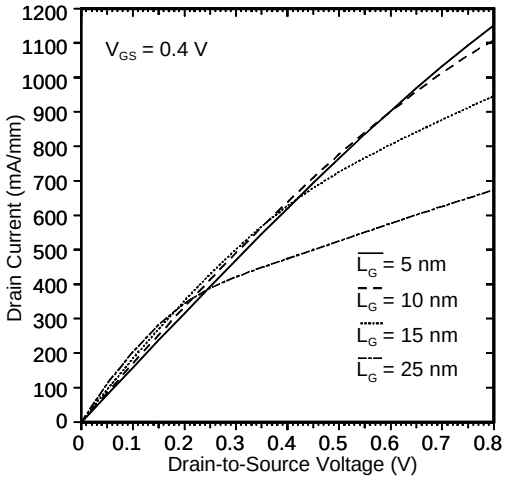

Figure 7: Single gate HEMT output characteristics for different gate lengths

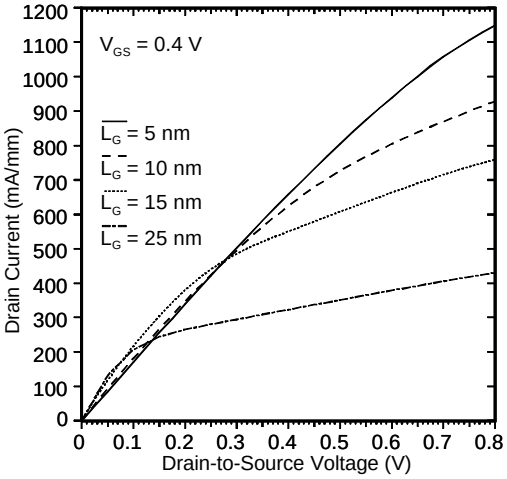

Figure 8: Striped-channel HEMT output characteristics for different gate lengths

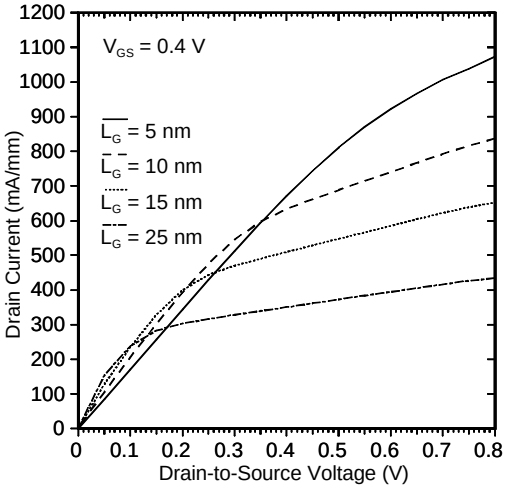

Figure 9: Double gate HEMT output characteristics for different gate lengths

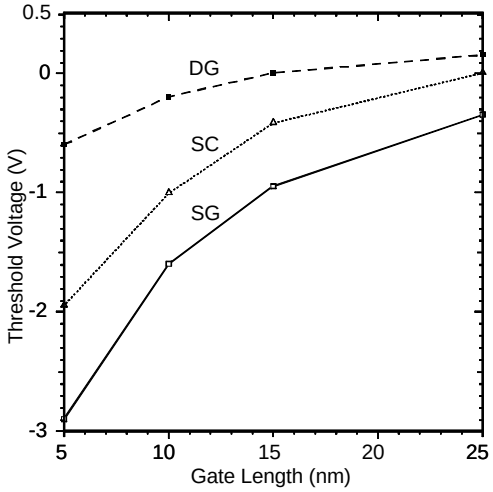

Figure 10: Threshold voltage for different gate lengths

The RF-results are summarized in Fig. 11. Reduced gate lengths results in increasing RF gains and consequently in increasing cut-off frequencies. At a gate length $L_G = 5$ nm transit frequencies of about 690 GHz, 790 GHz and 890 GHz can be attained with the single gate, striped-channel and double gate HEMT, respectively.

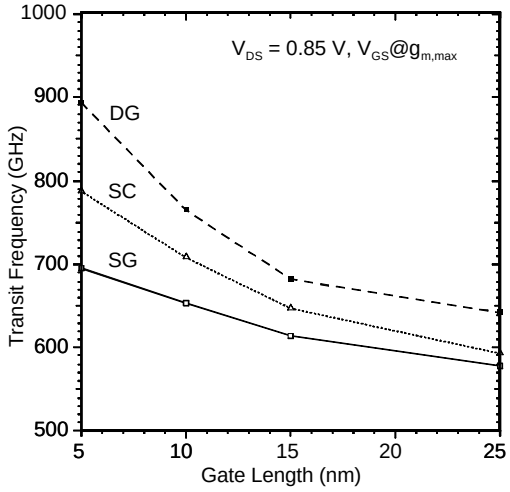

Figure 11: Transit frequencies for different gate lengths

For a further improvement of device performance a double pulse-doped layer structure with a gate length of 10 nm was investigated. The channel thickness was reduced to 10 nm. The sideway gate recess of the striped-channel device was increased to improve the control behavior of the lower electron gas. The drain current was increased by the factor 2.5 to 3 compared to the single pulse-doped structure. The increase of the transconductance by the factor 2.7 of the DG-HEMT is more significant as in the case of the SG and SC transistor (factor 1.3). As a consequence the DG device shows a more important rise of the RF-gains (see Fig. 12). The calculated transit frequencies are 1270 GHz, 860 GHz and 790 GHz for the DG, SC and SG-HEMT, respectively. So the devices have the capability for application in the THz range.

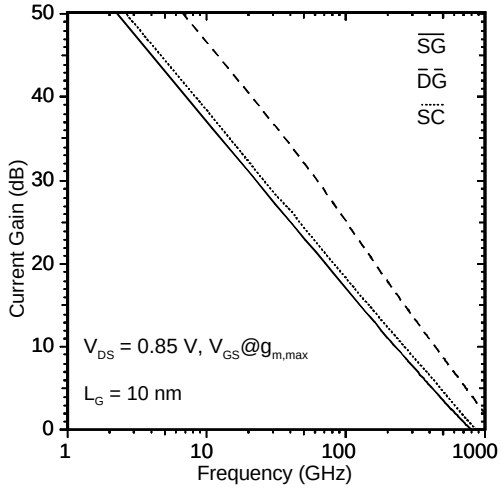

Figure 12: Current gain of double pulse-doped HEMTs

4. CONCLUSION

Numerical simulations of ultra-short channel HEMTs with single gate, striped-channel and double gate structures and gate lengths down to 5 nm have been carried out. Alternative gate concepts can reduce short channel effects and improve RF performance. Optimized double pulse-doped devices are able to work in the THz range.

REFERENCES

[1] Y. Yamashita, A. Endoh, K. Shinhara, K. Hikosaka, T. Matsui, S. Hiyamizua and T. Mimura, "*Pseudomorphic $In_{0.52}Al_{0.48}As/In_{0.7}Ga_{0.3}As$ HEMTs with an ultrahigh f_T of 562 GHz*", IEEE-EDL, 2002, **23**, pp. 573-575

[2] T. Schulz, W. Rösner, E. Landgraf, L. Risch and U. Langmann, "*Planar and vertical double gate concepts*", Solid-State Electronics, 2002, **46**, pp. 985-989

[3] Y. Kwon, D. Pavlidis, K. Hein and T. Brock, "*Striped-channel InAlAs/InGaAs HEMTs with shallow-grating structures*", IEEE Trans. ED, 1996, **43**, pp. 2046-2052

[4] W. Klix, R. Dittmann and R. Stenzel, "*Three-dimensional simulation of semiconductor devices*", Lecture Notes in Computer Science 796, Springer-Verlag, 1994, pp. 99-104

[5] J. Höntschel, R. Stenzel and W. Klix, "*Investigations of quantum transport phenomena in resonant tunneling structures by simulation with a novel quantum hydrodynamic transport model*, Proc.of 29th Int. Symp. on Compound Semiconductors (ISCS), Lausanne 2002

[6] B. Gonzalez, V. Palankovski, H. Kosina, A. Hernandez and S. Selberherr, "*An energy relaxation time model for device simulation*", Solid-State Electronics, 1999, **43**, pp. 1791-1795